MODELLING MOTION OF A TORSION OSCILLATOR: FINDING TORSION CONSTANT, DAMPING PARAMETERS, AND RESONANCE FREQUENCY

A PREPRINT

Nathan C. Pierce

Department of Physics (Undergraduate)

University of Michigan - Dearborn

4901 Evergreen Rd, Dearborn, MI 48128

piercen@umich.edu

March 19, 2021

ABSTRACT

In this experiment, the dynamics of motion of a torsion oscillator are observed, including free oscillations, underdamped and overdamped oscillations, and sinusoidal driven oscillations. Resonance of the oscillator is observed over a range of frequencies for such a driving force. Some physical parameters concerning these types of systems are determined, namely the torsion constant of the cable $\kappa = (0.052 \pm 0.002)\,\mathrm{N\,m\,rad^{-1}}$, a 'light' damping parameter $\gamma = 0.383 \pm 0.004$, a 'heavy' damping parameter $\gamma = 0.5 \pm 0.1$, and the natural frequency of the system is determined to be $f_R = (0.858 \pm 0.002)\,\mathrm{Hz}$. Instrumentation was employed to aid in the reduction of uncertainty (random error) in measurements made by the experimenter's senses. The experimental results agree with predictions made by oscillation theories in Newtonian mechanics.

1 Introduction

This experiment examines the properties of different kinds of simple harmonic oscillators. The TeachSpin torsional oscillator used in the experiment is an apparatus which allows modelling a variety of oscillators. The apparatus is constructed such that examinations of oscillators in a one-dimensional polar coordinate system are easily done.

The motion of harmonic oscillators is described by a sin function. A restoring force (modelled by Hooke's Law) acts on the oscillator and is opposite and proportional to the position of the oscillator i.e. the further the system is from equilibrium position, the greater the restoring force. In the experiment, the restoring force is the torque provided by the torsion fiber cable on the rotating body (a hub of various components). The hub is designed specifically such that no sliding contact occurs with the rotation of the rotor so that free oscillation can be observed for a long period of time. Measurements of angular position are taken directly from the rotating disc.

Dissipative or frictional forces constitute damping of an oscillator. In the experiment, damping of the torsion oscillator can be achieved by adjusting the location of magnetic disc brakes that surround the rotating disc. The brakes provide a static magnetic field for the rotor disc to move through. Eddy currents are induced in the copper as the rotor moves through the magnetic field, providing the damping force. The disc can be more or less immersed in the magnetic field by changing the position of the brakes, thereby increasing or decreasing the level of damping. Damping can also be done by adding weight to the taut lines that wrap around the rotor hub and attach to two pulleys on either side of the torsion oscillator. While the first method of damping described here is used to observe motion and find various damping parameters, the second method is used to find the torsion constant. Additionally, a sinusoidal driving force can be applied to the oscillator that varies harmonically with time.

The experiment covers a few 'sub-experiments' - first, the torsion constant of the steel torsion fiber is deduced by providing various torques to the torsion fiber via different hanging masses from the pulley system. The purpose of this experiment is primarily to get accustomed to working with the torsion oscillator and to become familiar with the different components of the apparatus.

Second, free and damped oscillations are observed - both angular velocity and angular position are plotted. Phase diagrams are generated from the displacement and velocity data (but are not included in the report as they are not considered critical to the discussion). The purpose of this experiment is to see the motion of an oscillator as a function of time, both by observing the physical system and by inspection of LabVIEW plots of these parameters, and to confirm predictions made by the theory of damped harmonic oscillators. Perhaps of more interest are the plots of damped oscillators, where the degree of damping depends (as a choice made in the experiment) on the position of the magnetic disc brakes relative to the rotating hub. Accord-

ing to the TeachSpin manual, the damping force generated by the eddy currents induced by the position of the magnetic dampers is proportional to the angular velocity of the rotor ($F_d \propto \alpha v^1$) The motion of damped oscillators is easy to inspect with the torsion oscillator and LabVIEW setup. Moreover, the damping parameter is deduced for two different levels of damping. Of the three general cases of underdamped oscillators (discussed in Sec 2), both underdamped and overdamped motion are observed - but the focus is placed on underdamped motion in the experiment. Lastly for this section, the natural frequency of the oscillator w_u is found.

Third, the oscillator is driven by a function generator signal over various frequencies that sweep over the resonance frequency, and the maximum amplitude for each frequency is recorded and plotted to find a relationship between driving frequency and maximum angular displacement. This component of the experiment is a study of resonance phenomena, and an exercise in data analytics to find the physical parameters from the data.

2 Theory

Simple harmonic motion occurs when a restoring force proportional to the distance from equilibrium acts on a body. The restoring force serves to bring an object back towards equilibrium. The restoring force is given by Hooke's Law:

$$\vec{F} = -k\vec{x} \tag{1}$$

The motion of such a system is harmonic - it is represented by a sin function, in its most simple form:

$$x(t) = Asin(\omega t - \delta) \tag{2}$$

From Newton's 2nd Law and Hooke's Law, the differential form of the harmonic oscillator is written:

$$\ddot{\theta} + \omega_u^2 \theta = 0 \tag{3}$$

Here $\omega_u^2 = \sqrt{\frac{k}{m}}$ is the natural frequency.

First consider the case when a damping force is acting on the oscillator. Then the differential equation is:

$$\ddot{\theta} + 2\gamma\dot{\theta} + \omega_o^2 \theta = 0 \tag{4}$$

Note that the damping parameter γ is a dimensionless quantity. If some damping is done on the oscillator and an oscillator driving force is added, then the motion can be deduced by solving the differential equation:

$$\ddot{\theta} + 2\gamma\dot{\theta} + \omega_o^2 \theta = Acos(\omega t) \tag{5}$$

The damped oscillator will show free, harmonic behavior for small t, but as $t \to \infty$, $x(t) \to 0$. The damped angular frequency, w_d, has meaning for the time period in which motion is oscillatory. If this motion is plotted, then it is enveloped by an upper and lower bound described by $x_{en} = \pm Ae^{-\gamma t}$ (see Fig. 1). The $e^{-\gamma t}$ term is called

the decrement of the motion. Since the motion is tending towards 0 with increasing time, energy must be lost in the form of heat or sound at a rate proportional to the velocity squared[1]. This rate of energy loss is maximum near equilibrium position, when the system attains its maximum velocity. Since real world systems tend toward the lowest energy state, physical oscillators are generally best approximated as underdamped. Then the rate of energy loss is proportional to the degree of damping, established by the damping parameter γ.

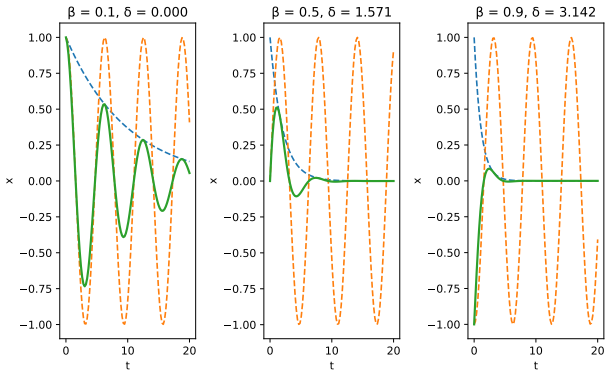

Figure 1. The oscillation of various systems with different damping parameters γ and phase angles δ. The dotted blue line is the decrement of the oscillator. The dotted yellow line is the free oscillator. The solid green line is the underdamped motion. The effects of different γ and δ are apparent.

In Eq. 5, the damping term is $2\gamma\dot{\theta}$ and the driving function is $Acos(\omega t)$. The solution to this equation is the sum of two solutions: the complementary solution $x_c(t)$ and particular solution $x_p(t)$. The complementary solution is the solution to the homogeneous second order ordinary differential equation above (when the right hand side is equal to 0), and has solutions in the form:

$$x_c(t) = e^{-\gamma t}(A_1 e^{\sqrt{\gamma^2-\omega_o^2}t} + A_2 e^{-\sqrt{\gamma^2-\omega_o^2}t}) \quad (6)$$

This is the solution to a damped oscillator without an external driving force - and is the complementary component of the solution to a damped oscillator $with$ a driving force. An underdamped oscillator satisfies the condition: $\omega_u^2 > \gamma^2$. For underdamped oscillation ($\omega_u > \gamma^2$), the motion is described by:

$$x(t) = Ae^{-\gamma t}cos(\omega_u t - \delta) \quad (7)$$

The damped frequency w_d is slightly less than the undamped frequency w_u by a factor:

$$\omega_d = \omega_u\sqrt{1-\gamma^2} \quad (8)$$

Finally, the particular solution is given by:

$$x_p(t) = \frac{A}{\sqrt{(\omega_o^2-\omega^2)^2+4\omega^2\gamma^2}}cos(\omega t - \delta) \quad (9)$$

Note that the ratio is the amplitude of oscillation. Since the motion is described by the sum of the solutions, the two components can be categorized by their behavior at various t. As $t \to \infty$, then $x_c(t) \to 0$, and the motion is entirely governed by $x_p(t)$, which is harmonic. The time period it takes for the complementary component of the motion

[1] *Classical Dynamics. Thornton, Stephen T., and Jerry B. Marion.*

to vanish is called the transient period. After $t_{transient}$, then the particular component of the equation of motion dominates. The time $t > t_{transient}$ is the steady state of the oscillator, and is purely harmonic.

To find resonance frequency, i.e. the frequency for which amplitude is maximum, we set the derivative of the ratio with respect to the angular frequency in Eq. 9 to zero, that is (setting the ratio equal to D):

$$\left.\frac{dD}{d\omega}\right|_{\omega=\omega_R} = 0 \tag{10}$$

ω_R could be deduced by collecting data of the maximum displacement angle θ_{max} for various driving frequencies.

For free oscillations with no damping: $\omega_o^2 = \frac{k}{m}$. For free oscillations with damping: $\omega_D^2 = \omega_o^2 - \gamma^2$. Note that $w_u > w_d > w_R$.

The degree of damping is often times described quantitatively by a 'quality factor' Q:

$$Q \equiv \frac{1}{2\gamma} \tag{11}$$

Where γ is the damping parameter. As Q increases, the more the oscillation models a free oscillator with no damping. Resonance can be destroyed for low Q, which requires damping large enough to drive the resonance amplitude curve to a flat line, as when $Q \approx 0$. Therefore, a $Q >> 0$ indicates that the system has minimal damping forces present. When investigating resonance, a large Q is preferred, otherwise the damping component of the differential equation will dominate over the driving force component. For damped systems, the three cases are:

1. Underdamped: $\gamma < 1$
2. Critically damped: $\gamma \equiv 1$
3. Overamped: $\gamma > 1$

3 Methods

3.1 Apparatus

To help isolate the system from any potential ambient vibration or noise, the whole torsion oscillator was placed on a rigid foam pad. Additionally, care was used throughout experimentation to prevent bumping the table which the apparatus sat on while data was being collected. Any unwanted energy added to the system would skew results. Further, when the level of tension in the torsion cable is appropriate, the cable can be plucked and a low musical tone will sound. This step was taken to ensure adequate cable tension.

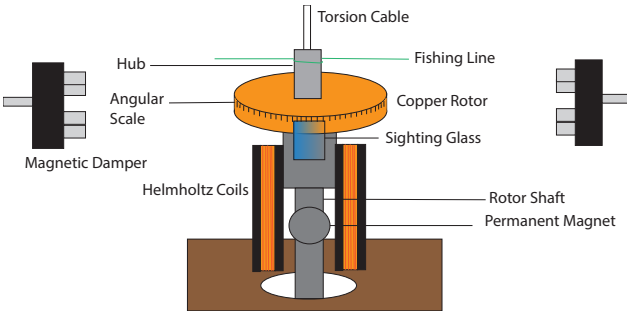

Figure 2. Line diagram of the apparatus hub. This diagram shows the upper half of the torsion oscillator apparatus. Below this, the torsion cable runs down runs down to the another clamp. The electrical connections are also at the bottom. The fishing lines run to the low friction pulleys on either side of the apparatus.

The primary component of the apparatus is the rotor hub. The hub line diagram can be seen in Fig. 2. The torsion cable runs the length of the apparatus from top to bottom. The cable runs through the rotor structure. The shaft is coupled to the cable at the hub. The rotor disc is made of pure copper, supported entirely by the tension in the fiber. The angular position transducer is at the bottom of the hub. Helmholtz coils are on either side of the hub. Eddy currents are generated in the copper rotor, which is used as one of the damping forces in the experiment (in finding the damping parameters). The currents are generated by the motion of the copper rotor through the static magnetic field created by the pair of magnetic disc brakes on either side of the rotor. Between the Helmholtz coils is a strong permanent magnet. Care was taken to keep magnetic materials from the permanent magnet to prevent damage. In front of the rotor is the plastic sighting glass. The rotor itself is marked in radians with major markings numbered $1.0 - 5.0$ rad.

The position of the magnetic disc brakes can be easily adjusted by thumbscrews on either side of the apparatus. On the bottom of the box are the electrical connections, including the power switch and BNC connectors for interfacing oscilloscopes or other devices, such as a National Instruments USB6009 DAQ used in the experiment. The BNC connections for angular position and velocity were wired in to a breadboard, and together with a ground connection, were then wired to the DAQ. The signal was sent through to two analog input channels on the DAQ. A two-voltage sensing LabVIEW program was used to monitor such properties of the system as the displacement and angular velocities over time, and phase diagrams were generated directly in the VI (virtual interface).

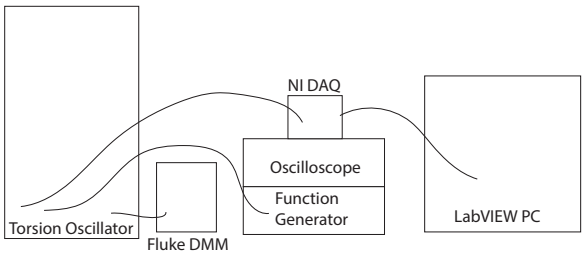

Figure 3. Schematic of the setup for the experiment. The USB DAQ was wired in to a breadboard, with BNC connections running from the base of the torsional oscillator. Only a voltage from the position transducer could be read while driving the oscillator with a signal from the signal generator. Otherwise, both velocity and position could be tracked.

3.2 Torsion Constant

To deduce the torsion constant κ for the cable, the disc brakes were positioned furthest away from the copper rotor. The damping effect of the brakes are negligible at the furthest position [2]. Torque was provided to the hub via a string (fishing line). The string wrapped around the hub and ran to a set of low-friction pulleys, one on either side of the apparatus. This ensures that the torque from the line is perpendicular to the radius of the hub. From the string, hangars were used to hang varying mass. The radius of the hub was measured with a set of Chicago brand calipers. Then, the net torque on the hub is $\tau_{net} = rg\sum_i m_i = -\kappa\theta$. Each hangar weighed $50\,\mathrm{g}$, and were weighed with an analytic balance as a check. Since the uncertainty of the calipers was $\delta r = \pm 0.05\,\mathrm{cm}$, the uncertainty of the hanging weight is neglected since δr dominates the quadrature sum ($\delta r > \delta m$) used to estimate the uncertainty in the torque. To prevent damage to the hub/fiber, no more than $400\,\mathrm{g}$ was added to either hangar at a time. Before the weight was added, the equilibrium position of the rotor θ_{eq} was measured.

The torsion constant κ was found using the relation $\kappa = \frac{\tau}{\theta} = \frac{rg\sum_i m_i}{\theta}$. By recording mass added to the hangar and knowing the radius of the hub, the torque is known. Then, the displacement of the rotor from equilibrium can also be recorded. The slope of the plot τ vs. θ yields κ.

[2] *TeachSpin, Torsion Oscillator Lab Manual*

3.3 Damping Parameters

The hanging weight method was used to find the torsion constant, but the magnetic disc brakes were used to find two different damping parameters γ. To find the damping parameter, first the natural frequency must be measured. The magnetic disc brakes were placed as far as they could from the rotor disc to reduce the damping parameter to a negligible degree, so that free oscillation could occur. The oscillation period T was collected both by hand and via the LabVIEW program, where analysis was done on the data to derive a frequency. When done by hand, the rotor disc was displaced $1.5\,\mathrm{rad}$ from equilibrium ($\theta_{eq} = 3.09\,\mathrm{rad}$) (note how θ_{eq} changed between experiments). The rotor was displaced from θ_{eq} by $1.5\,\mathrm{rad}$ to $\theta = 4.6\,\mathrm{rad}$ by hand, then let go. The time to complete a full oscillation was recorded with a stopwatch over four trials to find an average best value.

Finding a good position for the magnetic dampers proved to be challenging, as the degree of damping was extremely sensitive to the positioning of the dampers in relation to the copper disc. Some work was done to find a position that resulted in underdamping and not critical or overdamping. Having tabulated the natural frequency ω_o, the damping parameter could be obtained by measuring the period of oscillation with the damping force present, then solving $\gamma = \omega_o\sqrt{1 - (\frac{\omega_d}{\omega_o})^2}$. The period of oscillation T was again measured via a stopwatch and from data collected by the LabVIEW program. The first damping parameter

was found by adjusting the magnetic brakes such that the curved edge was roughly flush with the edge of the rotor disc. The second damping parameter was found when the curved edge of the disc brakes were roughly $\frac{1}{8}$ of the way over the edge of the disc. This approximate positioning of the disc brakes will prove to be problematic, as discussed later.

The next experiment required the use of a Rigol DG1022 function generator to provide a sinusoidal driving force to the oscillator. Data was collected for the first damping parameter γ_1 (with the disc brakes positioned approximately where they were when the parameter was tabulated). When a driving signal was applied to the system with the second damping parameter γ_2 configured, very little oscillation was detected, so no data was collected. This proved to be true over a sweeping range of frequencies, from $0.1\,\mathrm{Hz} - 1.3\,\mathrm{Hz}$. This interval includes the resonance frequency of the oscillator. However, even at the resonance frequency, very little oscillation was detected.

Data for the driving frequency was collected manually and automatically with the LabVIEW program. Measurement by hand proved to be difficult - especially near resonance, the maximum displacement position θ_{max} became very difficult to measure as the frequency increased. Care was taken to wait out the transient period between measurements, though validating the end of the transient proved difficult by eye and much easier programmatically, as any decay in the amplitude of the position vs. time plot is easy to spot.

Two different curve fitting routines were used in the analysis of collected data: one with Scipy's curvefit routine, and the other a custom Python fit parameter routine. The custom routine was used to generate a best guess of parameters that could then be passed to the Scipy routine to aid in the computation.

Figure 4. The setup for the experiment. On the left is the torsion oscillator. The middle section has a Keithley DMM (unused - the handheld Fluke 115 RMS DMM was used instead), Rigol Function Generator, and NI USB DAQ with breadboard. The oscillscope is just to the right of these. Off frame to the right is the PC used to run the LabVIEW program. Note the magnetic dampers are currently not attached to the torsion oscillator, but they can be seen at the bottom left of the frame. Also note the foam pad under the oscillator, used to help isolate the system from noise.

4 Results and Discussion

4.1 Torsion Constant

Determining the torsion constant κ required measuring the radius of the hub, found to be $(1.13 \pm 0.05)\,\mathrm{cm}$ by

measuring with a caliper. Not all of the masses added to the hangar to produce torque were measured on a scale - however, both hangars were confirmed $m_{hangar} = 50\,\mathrm{g}$ by weighing on an analytic balance. The uncertainties in the weights of the masses were assumed negligible.

The torsion constant κ was found to be $0.0517\,\mathrm{N\,m\,rad^{-1}}$. This constant can be related to more fundamental parameters, such as the twisting of two sections of the fiber and the the radius of each twisted fiber r. Visual inspection of the data shows a linear trend in θ vs. τ.

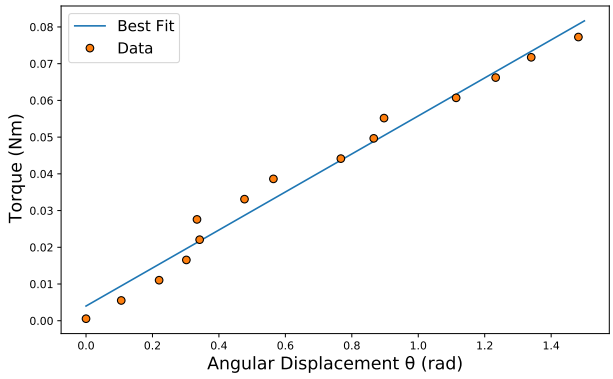

Figure 5. The data and fit for the Torsion constant. $\kappa = 0.0517\,\mathrm{N\,m\,rad^{-1}}$ The counter torque (counter to the torque provided by the torsion cable) is provided by hanging mass to a fishing line that wraps around the hub above the rotor.

4.2 Free and Damped Oscillation, Damping Parameters

To observe free oscillation, the magnetic disc brakes were set as far from the rotor as possible. In hindsight, the brakes should have been totally removed from the apparatus. As will be discussed, the damping parameter γ is non-zero with the brakes at this position. Despite the TeachSpin manual suggesting that the magnetic brakes could be situated to result in negligible damping, the ease of removing the magnets via two thumbscrews constituted the additional step to minimize damping. In retrospect, this should have been done.

To find the damping parameter, all that is needed is the natural frequency w_u and the damped frequency w_d of the oscillator. Then Eq. 8 can be solved for γ. In finding the natural frequency f_o of the rotor, the period measured by eye was found to be $T_{u,hand}(1.1 \pm 0.2)\,\mathrm{s}$ (the subscript denotes the method used to arrive at the value), yielding an angular frequency $\omega_{u,hand}(5.7 \pm 0.4)\,\mathrm{rad\,s^{-1}}$. The contribution of random error to the uncertainty in measuring the period is significant - and is largely associated with reflex time (measurements of period were taken with a stopwatch by visual inspection of the system in motion). To aid in the reduction of this uncertainty, LabVIEW data was collected and then analyzed. The virtual interface allowed for setting the sample rate (in hz) and the total sampling time and thus a total number of data samples. These settings were adjusted to collect 4000 samples over $20s$ for the undamped motion and $5s$ for the damped motion. The longer period for the undamped was to ensure the amplitude was constant throughout time, and the shorter period for the damped because that is about the lifetime of the transient period, before the amplitude goes to 0.

By running the data through a curve fitting routine (Scipy curvefit), best-fit parameters were generated. Then the equation for damped motion (Eq. 6) was plotted with the

parameters, and the data plotted against it (see Fig. 6). Initially, the equation for free-harmonic motion was used (Eq. 2), but the damped equation of motion better fit the data (Eq. 6). This would make sense - some level of damping should be expected, since the magnetic brakes were not removed. The damping parameter produced by the curve-fit is $\gamma = 0.012$. There is a minor discrepancy between the data and the fit at the peaks - indicating that the fit does not produce an accurate gamma. By inspecting Fig. 6, the discrepancy is greatest at low t, and is reduced at larger t. The fit overestimates the peaks at lower time. This relationship between the discrepancy in peak amplitude over time suggests the time pre-factor (γ) is off - this checks out with Eq. 6. Ultimately, the gamma would be off only by a small amount - and the model does fit the data very well when accounting for the other three parameters (A, ω_u, δ).

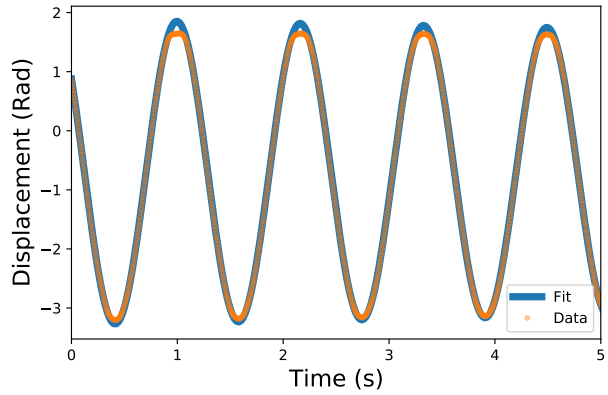

Figure 6. Motion of the copper rotor was measured as a function of time. Note the discrepancy in the fit to the data at the peaks for low t, and how the discrepancy is reduced at larger t. Data was collected from LabVIEW by measuring voltage in the angular position transducer on the apparatus. $A = -2.583$, $\gamma = 0.012$, $\omega_u = 5.39$, $\delta = 2.23$ (phase shift)

By using the instrumentation described in Sec. 3, uncertainty is markedly improved. From the LabVIEW/analysis technique, the period for the undamped oscillator under this configuration was found to be $T_{u,LV} = 1.165\,\mathrm{s}$ (where the subscript indicates that the LabVIEW method was used). Then, the angular frequency can be directly calculated ($\omega = 2f\pi = \frac{2\pi}{T}$). In this case, the rotors natural angular frequency was found to be $w_{u,LV} = 5.392\,\mathrm{rad\,s^{-1}}$. As can be seen, the values for these parameters calculated from the "free hand" observations differ from those generated via the LabVIEW/data analysis method. Because of the reduction in random error, these values are the preferred result from the natrual frequency experiment.

This process was repeated for the damped oscillator. As previously mentioned, two 'damped' experiments were performed - one lighter, and one heavier. The heavier damping force proved to overdamp the system such that no oscillation resulted.

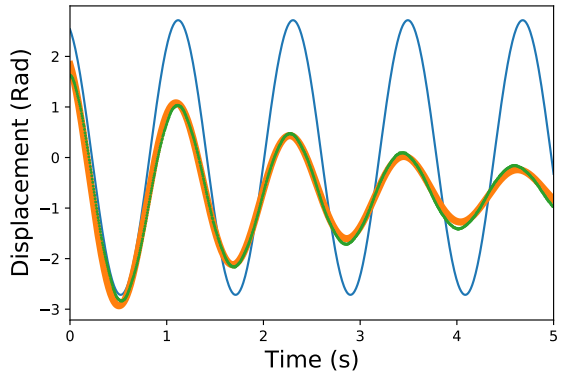

Figure 7. A plot of the motion of the central hub of the apparatus over time. The data (green) are points that lie almost entirely along the best fit line. The orange line is the best fit, and the blue line is the harmonic at this amplitude, phase angle, and frequency. This illustrates the decreasing amplitude of the damped oscillator over time. For the damped oscillator, $A = -2.71$, $\gamma = 0.383$, $\omega_d = 5.337$, $\delta = 2.774$

Since no oscillation was observed with the heavier damping parameter configuration, the resonance portion of the experiment was bypassed for this γ_2 value. Instead, the focus of the resonance experiment was placed on the lighter damping parameter. The TeachSpin manual suggested that a $Q_{ideal} \approx 8$ should be used when investigating resonance. The heavy damped parameter $\gamma_{H,hand} = 0.471$ results in a $Q \equiv 4.25$ - evidently the difference $\Delta Q = Q_{ideal} - Q_{measured}$ is enough to separate a workable investigation of resonance from one which has almost no oscillation. At the time of experiment, the suggestion regarding the Q value was not known, otherwise this trial would not have been attempted, and instead a trial with a lower damping parameter γ would have been run.

The damped motion parameters were found with the same data analysis technique used in finding the physical parameters for the free harmonic motion, $\gamma_{LV} = 0.383$, with $Q \approx 5.22$. While still less than the ideal Q value, investigating resonance at this damping constant was feasible. The plot of the motion of the oscillator at this magnitude of damping yields characteristic underdamped motion (see Fig. 7). In this case, $T_d, LV = 1.177\,\mathrm{s}$ and $w_{d,LV} = 5.337\,\mathrm{rad\,s^{-1}}$. As theory would predict (Eq. 8), $w_d < w_o$. The damped period measured with a stopwatch was found to be $T_{d,hand} = (1.2 \pm 0.2)\,\mathrm{s}$, and $w_{d,hand} = 5.193\,\mathrm{rad\,s^{-1}}$. The values determined from the electronic data acquisition system are held with higher confidence because of the decreased uncertainty and because of the number of sample points from which the best value was derived. Furthermore, inspection of Fig. 7 shows how well the curve-fit routine fit parameters (being supplied to the theoretical equations) accurately models the data. The model was (again) the damped harmonic motion Eq. 6.

	Undamped	Damped
$\omega(\frac{rad}{s})$	5.392 ± 0.002	5.34 ± 0.02
$T(s)$	1.165 ± 0.002	$1.177\ 1.18 \pm 0.02$
γ	0.012 ± 0.004	0.383 ± 0.004

TABLE I. Summary of parameters (with uncertainty) used in determining the damping parameter (γ) for two different levels of damping ('undamped' had the magnetic brakes as far back from the rotor as they could go - 'damped' had them closer, flush with the rotor edge). Values were determined initially by hand - resulting in high random error. The values presented here are determined from the analysis of data collected through a LabVIEW data acquisition configuration.

Both of the methods (by hand or via analysis of LabVIEW data) agree with one another - that is, the values determined lie within the error of the "by hand" calculations. See Table *I* for a synopsis of the experimental results with uncertainty.

4.3 Resonance

For the driven resonance section of the experiment, the magnetic disc brakes were returned to the same (approximate) position as the 'light damping' section. That is - the inner, concave edges of the disc brakes were flush with the outer, convex edge of the rotor. A range of driving frequencies was swept over to drive the oscillator, from 0.1 Hz to 1.3 Hz.

There were two methods used to collect data for resonance - the first was to visually wait out the transient period and then use the sighting glass to measure the maximum displacement angle as the rotor was rotating. This method turned out to be crude and ineffective - at best (at driving frequencies on the far end of either side of the resonance frequency), the measure of amplitude was approximate. At worst (near resonance), taking even a rough estimate of the amplitude became impossible, as there was no reliable way to take an accurate reading with the rotor rotating so quickly. Upon realization of this, the two-voltage LabVIEW program was again utilized to collect data. Without the plot of the motion provided by the program, waiting out the transient period to take a measurement became a matter of guesswork. Utilizing the displacment vs. time plot made waiting out the transient easy - one only had to wait for the motion to resemble perfect harmonic motion, with a constant amplitude over all time.

Displacement vs. time data was collected for driving frequencies between $0.1 - 1.3$ Hz over 0.1 Hz intervals. The data was filtered to extract the maximum amplitude for each driving frequency, using a simple for loop and numpy functions. Once the maximum amplitude was plotted against driving frequency, it became clear that more data points were needed near resonance, as the amplitude near resonance changes exponentially. More data near resonance was collected to aid in producing fit parameters to model the data against. In this case, the solution to the particular ODE Eq. 9 was used to fit the data. Fitting the data gives $C = 1.41$, $f_o = 0.862$, and $\gamma = 0.071$. This results in a Q value of 7.04. This is closer to $Q_{ideal} \approx 8$, but is

unexpected - after all, the magnetic brakes were positioned at about the same place as when the light damping parameter was found, so the damping parameter should be similar to $\gamma = 0.383$. Such a large difference in γ over such a small perceived difference in position of the dampers suggests that the damping force is extremely sensitive to the position of the dampers, i.e. even a small adjustment to the position results in a large change in γ.

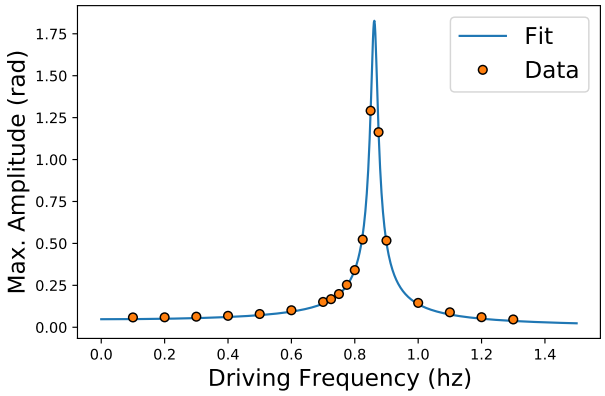

Figure 8. Damped driven oscillation. Driving frequency was swept over evenly spaced intervals until it was noticed that the data does not well define the peak. Even after collecting more data near the resonance peak, the fit is poorly defined for the peak value. The peak lies between the $f = 0.85$ Hz and $f = 0.875$ Hz frequency data points. Fit parameters are $C = 1.41, f_o = 0.862, \gamma = 0.0.071$ (fitting function is Eq. 9).

A quick look at the result, Fig. 8 shows that the data curve is poorly defined near the peak (near resonance frequency). The graph suggests that the resonance frequency f_R is somewhere between the two data points at $f = 0.85$ and $f = 0.875$. This is what we ought to expect - given the natural frequency of the oscillator was found to be $\omega_u = (5.392 \pm 0.002)\,\mathrm{rad\,s^{-1}} \rightarrow f_R = (0.858 \pm 0.002)\,\mathrm{Hz}$. Based on the model acquired from the data, the maximum amplitude of the fit curve occurs at $f = 0.861$ Hz - quite close to the predicted resonance. Considering how well the data is fit by the model (with exception near the peak amplitude), this is likely a good estimate, and agrees with the frequency of the oscillator found with minimal damping. Furthermore, we can see that the derivative of this curve of the maximum amplitude is equal to 0 when the driving frequency is equal to the resonance frequency, just as Eq. 10 predicts.

5 Conclusion

Based on these results, it can be said that predictions of the behavior of oscillating systems are confirmed experimentally, i.e. the current understanding of Newtonian mechanics accurately predicts the motion of an oscillating system over time - for oscillators that are: (approximately) free of forces, have some damping forces present (for damping forces proportional to the velocity of the oscillator), and those that have some external sinusoidal force being applied to them. Furthermore, some resonance phenomena was observed, and it was indeed discovered that the derivative of the amplitude curve as a function of frequency is 0 when the frequency is equal the resonance frequency of the oscillator (Eq. 10). Finally, the heavy reliance on the equations to model the data resulted in best-fits that matched the data very well, indicating the validity of the theory for this particular physical configuration.

To summarize the parameters found once more, the torsion constant was found to be $\kappa = (0.052 \pm 0.002)\,\mathrm{N\,m\,rad^{-1}}$, the 'light' damping parameter $\gamma = 0.383 \pm 0.004$, the 'heavy' damping parameter $\gamma = 0.5 \pm 0.1$, and the natural frequency of the system was determined to be $f_R = (0.858 \pm 0.002)\,\mathrm{Hz}$.

There were some flaws in the experimental procedure, namely: selecting a damped oscillator with a poor Q value, not entirely removing the magnetic brakes when modelling free oscillation, relying on human senses to collect data for such an experiment (although, this flaw was recognized and carried in the course of the experiment), and not collecting more data near the resonance frequency for the resonance sub-experiment. Perhaps the biggest inconsistency is in the positioning of the dampers - the position should not have been adjusted at all. Instead, a position with an appropriate Q value should have been found, and any data needing to be collected at that position should have been taken all at once. Only then should the magnetic brakes be moved. Otherwise, very careful measurement of the exact position of the brakes could have been used, as opposed to the guesswork done here. Despite these flaws, the experiment was a success.

References

[1] *"TeachSpin Torsion Oscillator." 1 June 2011, pp. 3–1*

[2] *Thornton, Stephen T., and Jerry B. Marion. Classical Dynamics of Particles and Systems. 5th ed., Cengage Learning, 2014.*